Proc. Natl. Acad. Sci. USA
Vol. 80, pp. 7118–7122, December 1983
Biochemistry

Activation of the c-*mos* oncogene in a mouse plasmacytoma by insertion of an endogenous intracisternal A-particle genome

(cellular oncogene/endogenous retroviruses/transposition/repetitive cellular elements)

E. CANAANI, O. DREAZEN, A. KLAR, G. RECHAVI, D. RAM, J. B. COHEN, AND D. GIVOL

Department of Chemical Immunology, The Weizmann Institute of Science, Rehovot 76100, Israel

Communicated by Michael Sela, August 16, 1983

ABSTRACT **The activation of the cellular oncogene c-*mos* in mouse plasmacytoma XRPC24 was found to result from the insertion of a 4.7-kilobase-pair cellular DNA element, within the c-*mos* coding region. The element terminates on both sides with a direct repeat of around 335 nucleotides. The repeat as well as internal sequences of the element show strong homology to endogenous intracisternal A-particle (IAP) genes. The IAP genome integrated within c-*mos* in a head-to-head (5′ to 5′) configuration. This juxtapositioned the IAP 5′ long terminal repeat next to the bulk of the oncogene's coding region and shifted c-*mos* 5′ coding and flanking sequences to a position further upstream. The significance of several aspects of this activation and transposition event is discussed.**

c-*mos* is a member of the family of cellular sequences, termed *onc* genes, which possess the potential to become malignant through incorporation into the genome of retroviruses (1) or by undergoing alterations within the cell (2). c-*mos* is the progenitor of the transforming information (v-*mos*) in Moloney murine sarcoma virus. The virus is presumably a recombinant between Moloney murine leukemia virus and the c-*mos* gene of BALB/c mice (3, 4). c- and v-*mos* are composed of nearly identical sequences over their coding region, with the exception that c-*mos* contains 21 additional codons at the 5′ terminus, substituted in v-*mos* with 5 codons derived from viral helper sequences (5, 6). A M_r 37,000 protein identified within virus-infected cells (7) is encoded by the 374 codons of v-*mos* and presumably triggers cellular malignant transformation. No homologous protein coded by c-*mos* has been detected in normal cells.

In a recent study (8) we described the rearrangement of the c-*mos* gene in mouse plasmacytoma XRPC24. Sequences from the 5′ region of the gene, including 264 nucleotides of the presumed *mos* coding sequence as well as 5′ flanking DNA, were substituted with a unique DNA. This rearrangement was accompanied by the appearance of *mos* transcripts in the tumor. Moreover, the molecularly cloned rearranged gene (termed rc-*mos*), unlike its normal counterpart, induced transformed foci upon transfection into NIH/3T3 monolayers.

More recently it was shown (9) that a 0.35-kilobase-pair (kbp) segment of the unique DNA, immediately adjacent to the junction point with c-*mos* sequences retained in rc-*mos*, had 88% sequence homology with the long terminal repeat (LTR) of an endogenous genetic element molecularly cloned from a library of mouse DNA (10). This element is a member of a family of highly reiterated endogenous mouse genes [intracisternal A particle (IAP) genes] homologous to the RNA of IAPs. The latter are noninfectious retrovirus-like structures found regularly in early mouse embryos (11–13) and present abundantly in every mouse plasmacytoma (14) and other mouse tumors (15).

The association between an IAP LTR and the rearranged cellular *mos* was of considerable interest because it constituted one example of activation of a cellular oncogene by a mechanism involving relocation of endogenous sequences. Therefore, we considered it important to resolve several questions related to this mechanism. First, did the activation involve insertion of a partial IAP genome—possibly a single LTR—or did it involve a complete genome? Second, were the 5′-terminal c-*mos* and flanking mouse sequences deleted during the rearrangement process? In this paper we show that a 4.7-kbp IAP genome containing two LTRs was inserted within c-*mos*. This juxtapositioned the IAP 5′ LTR next to the main coding body of the oncogene and the 3′ LTR next to c-*mos* 5′-terminal codons. The insertion also caused a duplication of six c-*mos* nucleotides at both ends of the IAP genome.

MATERIALS AND METHODS

Restriction Enzyme Analysis. High molecular weight cellular DNA and phage DNA were digested with restriction enzymes (New England BioLabs) according to the protocols of the manufacturer. Electrophoresis on agarose gels, blotting, and hybridization in a buffer containing 50% formamide to nick-translated probes were performed as described (8, 16).

Molecular Cloning. rc-*mos* *Eco*RI DNA fragment was enriched from XRPC24 DNA by electrophoresing 300 μg of digested DNA on a 0.5% agarose gel. After identification of the fragment by blotting and hybridization of a longitudinal slice of the gel, the DNA was eluted from the corresponding region on the remainder of the gel by absorption to glass beads (17). The eluted DNA was cloned into λ *Wes*B (18) DNA arms, and plaques containing c-*mos* information were identified and purified as described (19).

DNA Sequence Analysis. Two fragments containing 5′ rc-*mos* information were subjected to sequence analysis. The *Ava* I–*Ava* I fragment was labeled at both ends by using reverse transcriptase. The strands were separated and subjected to sequence analysis by the Maxam and Gilbert method (20). The *Pst* I–*Pst* I fragment was cloned into M13 phage and two phages with inserts in opposite orientation were subjected to sequence analysis by the chain termination method (21).

RESULTS

Identification of the 5′ rc-*mos* Sequence in XRPC24 Tumor DNA. Our previous work has identified in XRPC24 plasmacytoma DNA two *Eco*RI fragments containing c-*mos* sequences (8). These included a 14-kbp fragment corresponding to the normal gene (22) and a 12-kbp rearranged gene, which we termed

The publication costs of this article were defrayed in part by page charge payment. This article must therefore be hereby marked "*advertisement*" in accordance with 18 U.S.C. §1734 solely to indicate this fact.

Abbreviations: kbp, kilobase pair(s); LTR, long terminal repeat; IAP, intracisternal A particle.

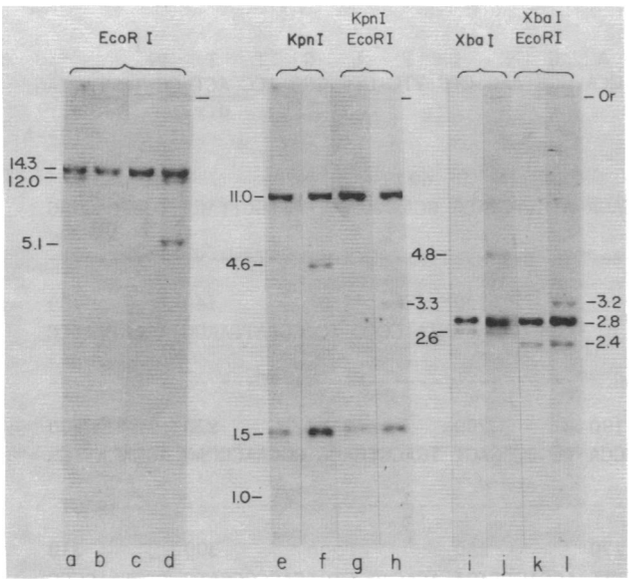

FIG. 1. Southern blot analysis of *mos* sequences in BALB/c and XRPC24 DNA. Ten-microgram aliquots of high molecular weight DNA of BALB/c mouse (lanes b and c) and XRPC24 plasmacytoma (lanes a, d, and e–l) were digested with restriction enzymes (detailed in figure), electrophoresed on 0.7% agarose gels, and, after blotting onto nitrocellulose filters, screened by hybridization with radiolabeled 3′ *mos* probe (lanes a, b, e, g, i, and k) or total *mos* probe (lanes c, d, f, h, j, and l). Size markers are given in kbp. Note that the 1.5-kbp *Kpn* I band consists of two fragments, only one of which is digested with *Eco*RI into a 1-kbp fragment. Or, origin.

rc-*mos*. The latter was composed of all c-*mos* sequences 3′ to codon 87 as well as a unique DNA substituting the sequences 5′ to this point. The probe used in these experiments was a *Bgl* I–*Hin*dIII 0.9-kbp v-*mos* fragment (6), which corresponded to the 3′ 294 codons of c-*mos* (5) but lacked, and therefore could not detect, the 5′ 87 codons of the gene. We repeated these experiments using this probe as well as a radiolabeled *Xba* I–*Hin*dIII v-*mos* fragment (6) subcloned from Moloney murine sarcoma virus DNA into pBR322 plasmid. This fragment spans and can detect all of c-*mos* coding sequences except for the 5′-terminal 21 codons. Hybridization of each probe to Southern blots of BALB/c mouse DNA digested with *Eco*RI revealed the expected 14-kbp c-*mos* band (Fig. 1, lanes b and c). In a similar analysis with XRPC24 DNA, the *Bgl* I–*Hin*dIII radiolabeled probe detected the 14-kbp fragment as well as the 12-kbp rc-*mos* (Fig. 1, lane a). Hybridization of the tumor DNA with the *Xba* I–*Hin*dIII probe revealed an additional 5.1-kbp *mos* fragment (Fig. 1, lane d). The detection of the 5.1-kbp fragment only by a probe containing 5′-terminal *mos* information suggested that it corresponded to the "missing" 5′ segment of c-*mos* severed away from the rest of the gene (rc-*mos*) by insertion of IAP-related DNA.

The topography of this 5′ segment of c-*mos*, which we now term 5′ rc-*mos*, with respect to the remainder of the gene (previously called rc-*mos* and now retermed 3′ rc-*mos*) was studied by performing a series of restriction enzyme digestions of XRPC24 cellular DNA and identifying *mos*-containing fragments by Southern blot hybridization. In each case the blots were hybridized first to the *Bgl* I–*Hin*dIII radiolabeled DNA fragment that detects 3′ rc-mos and then to the *Xba* I–*Hin*dIII DNA probe that detects both 3′ and 5′ rc-*mos*. Representative results are shown in Fig. 1. Thus, a 3′ rc-*mos Kpn* I fragment of 1.5 kbp (apparent in Fig. 1, lane e) is cut into a 1.0-kbp 3′ rc-*mos* DNA after digestion with *Eco*RI (Fig. 1, lane g). Similarly, a 2.6-kbp *Xba* I 3′ rc-*mos* fragment (Fig. 1, lane i) is split after *Eco*RI digestion into a 2.4-kbp *mos* DNA (Fig. 1, lane k). This places *Xba* I and *Kpn* I sites 0.2 and 0.5 kbp, respectively, 5′ to the terminal left *Eco*RI site of 3′ rc-*mos* (see Fig. 2). Similar analysis using the *Xba* I–*Hin*dIII DNA probe identified fragments containing 5′ rc-*mos* information. A 4.6-kbp *Kpn* I fragment (Fig. 1, lane f) was cut with *Eco*RI into a 3.3-kbp segment (Fig. 1, lane h), and a 4.8-kbp *Xba* I fragment (Fig. 1, lane j) was digested with *Eco*RI into 3.2-kbp DNA (Fig. 1, lane l). These results placed *Kpn* I and *Xba* I sites 1.3 and 1.6 kbp, respectively, downstream from the 3′ *Eco*RI site of 5′ rc-*mos* (see Fig. 2). It also suggested that the *Kpn* I and *Xba* I sites detected by the two probes are identical and reside on another 1.7-kbp *Eco*RI fragment separating 5′ and 3′ rc-*mos* (Fig. 2). This conclusion was further corroborated by Southern blots of *Xho* I, *Bam*HI, and other enzyme digests (not shown). The results of this analysis allowed us to draw a map of the rearranged c-*mos* gene (Fig. 2). The map demonstrates that c- and rc-*mos* are identical in the flanking regions. rc-*mos* originated by the insertion of a 4.7-kbp unique DNA and splitting of c-*mos* into two segments.

5′ rc-*mos* Contains an IAP LTR. To study further the DNA inserted between the two regions of c-*mos*, we molecularly cloned the *Eco*RI 5.1-kbp 5′ rc-*mos* fragment from XRPC24 DNA. The fragment was enriched by preparative agarose gel electrophoresis and then cloned into λ *Wes*B vector (18). Initial hybridization experiments indicated that the cloned DNA cross-hybridized with the IAP LTR present at the 5′ end of 3′ rc-*mos* (not shown). To examine the extent of this homology a portion

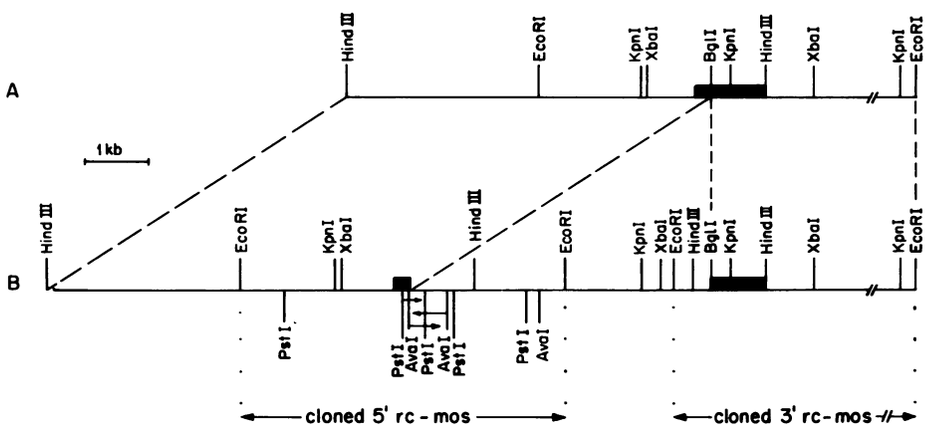

FIG. 2. Physical maps of c-*mos* (*A*) and rc-*mos* (*B*) loci. Black boxes denote coding regions. Arrows drawn near the 5′ rc-*mos* coding region show the strategy of the nucleotide sequence analysis. The area bound by coding regions in rc-*mos* corresponds to the inserted IAP genome. kb, Kilobase.

```
                PstI                    AvaI
                 C   S   I   P   L   V   A   P   R   K   A   G   K   L   F   L   G   T   T   P↓1
5' rc-mos       C TGC AGC ATT CCT TTG GTG GCC CCG AGG AAG GCA GGG AAG CTC TTC CTG GGG ACC ACT CC TGTTACTAG
                                                                                    d.r.
3' rc-mos                                                                                       -----T---A

                10          20          30          40          50          60          70          80
5' rc-mos       CGTTCTCCAC G CCGGCCAG GAAGAACACA GCAAACCAGA ATCTTCTGCG GCAAAACTTT ATTGCTTACA TCTTCAGGAG

3' rc-mos       CG------- -- -A-------- ---------C A--G------ ---------- -----G---- ---T------ ----------

                 90         100         110                         120         130         140         150
5' rc-mos       CAAGAGTGTA AGAAGCAAGA GAG                       CGAGAAAACG AAACCCCGTC CCTATTAAGG AGAATTATCC

3' rc-mos       -C--G--CG- G--------- ---CAAGAAG CAAGAGAG   ---------- ---------- ---C------ --C---C---

                       160         170         180  PstI  190         200         210         220         230
5' rc-mos       TTCCCCTAGC AGGTGTCACT CCCTGATTGG CTGCAGCCCA TCGGCCGAGT TGACGTCACG GGGAAGGCAG AGCACATTGA

3' rc-mos       ---G---C-G -C-------- ---------- -------- - ------ --- ---------- ---------- ------AGT-

                       240         250         260         270         280         290         300         310
5' rc-mos       GTGAGAACCT ACCCTCGGCA CATGCGCAGA TTATTTGTTT ACCACTTAGA ACACAG CTGTCAGCGCCATC TTGTAACCGG

3' rc-mos       --C-T--GA- -----T---- ---------- ---------- ---------- ------GA------------ ----- ----

                       320         330      ↓  340         350         360         370         380         390
5' rc-mos       CGAATGTGGG GGCGGCTCCC AACACTCCCC CTTTTCTTTT AATAAGAGCA AATAGGCCAC CCATATTAAT AGAGAGTGGA
                                        ◣     T P   P R A   P
3' rc-mos       ---------- C--------- ----CACTCC TCCTCGGGCT CCC
                                        d.r.
```

FIG. 3. Nucleotide sequence of the two termini of the 4.7-kbp DNA inserted within c-*mos*. The sequences delineated by vertical arrows represent IAP LTRs. Note that *mos* codons 5′ to the top arrow in 5′ rc-*mos* and 3′ to the bottom arrow in 3′ rc-*mos* are joined in the nonrearranged c-*mos*. d.r., Direct repeat; corresponds to duplication of six nucleotides of *mos* sequence during IAP integration. Underlying arrows represent the inverted repeat of an IAP LTR. Amino acids of c-*mos* are given in a single-letter code (23) above the nucleotide sequence.

of 5′ rc-*mos* was subjected to sequence analysis according to the strategy depicted in Fig. 2 (see also *Materials and Methods*). This sequence and the IAP LTR of 3′ rc-*mos* were aligned and are shown in Fig. 3. Both are drawn in the 5′ to 3′ direction with respect to c-*mos* transcription. However, it should be noted that with regard to normal transcription of the IAP genome, it is the anti-sense strand of the LTR that is shown here (24).

The LTR within 5′ rc-*mos* is preceded by the first 86 codons of c-*mos*, whereas the LTR in 3′ rc-*mos* is followed by the bulk of the coding region. Six nucleotides of c-*mos* at the junction point with the LTR are duplicated (marked in Fig. 3 as d.r., direct repeat). Each LTR terminates in a short inverted repeat (underlined in Fig. 3). The 335 nucleotides of the 5′ rc-*mos* LTR match the 3′ rc-*mos* LTR in 307 (92%) places. There are 28 mismatches, four insertions, and four gaps in the 5′ rc-*mos* LTR. One of these gaps consists of a stretch of 15 nucleotides previously identified as an internal duplication in 3′ rc-*mos* (9) and noted to be absent in the LTR of the cloned IAP genome MIA14 (9). These studies establish that the 4.7-kbp DNA inserted within c-*mos* ends on both sides with IAP LTR.

The 4.7-kbp DNA within c-*mos* Is an IAP Genome. To examine if the non-LTR sequences within the 4.7-kbp DNA placed within c-*mos* are of IAP origin, we tested a non-LTR segment of 5′ rc-*mos* (the 3′-terminal *Hin*dIII–*Eco*RI fragment) for hybridization to endogenous IAP sequences distributed within the mouse genome (10, 25). Southern blots of *Eco*RI- and *Hin*dIII-digested BALB/c DNA were probed for IAP-specific fragments by hybridization to non-LTR probes from a typical IAP genome, pMIA1 (10), and from 5′ rc-*mos*. The *Eco*RI–*Hin*dIII combination was chosen because these enzymes recognize conserved sites within IAP genomes and produce a characteristic pattern of reiterated internal fragments (10, 25). Indeed, the pMIA1 probe detected an extensive array of IAP fragments ranging in size from 0.5 to 6.0 kbp (Fig. 4, lane a). The 5′ rc-*mos* probe cross-hybridized with most of these fragments although with some difference in intensity (Fig 4, lane b). These

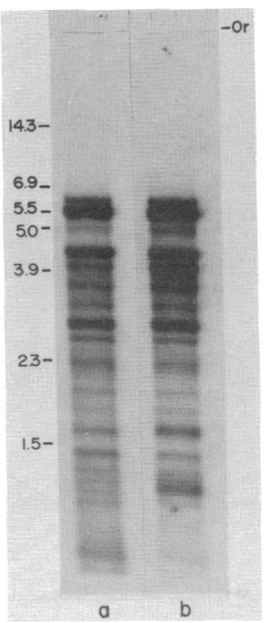

FIG. 4. Southern blot analysis of BALB/c mouse DNA examining hybridization to non-LTR probes derived from the pMIA1 IAP genome (10) (lane a) and the 4.7-kbp DNA inserted into c-*mos* (lane b). Ten-microgram aliquots of high molecular weight DNA digested with *Eco*RI and *Hin*dIII were analyzed as described in the legend to Fig. 1. The probe derived from rc-*mos* corresponds to the *Hin*dIII–*Eco*RI 3′ terminus of 5′ rc-*mos*. Size markers are given in kbp. Or, origin.

results indicate that the sequences bound by the LTRs of the 4.7-kbp inserted element are homologous to IAP sequences. Direct evidence that the 5′ rc-*mos* clone contains an IAP genome was obtained by hybridization of the same probe (the 3′-terminal *Hin*dIII–*Eco*RI fragment of 5′ rc-*mos*) to plasmid pMIA1, which contains only the body of IAP without LTR (10). After digestion of pMIA1 with *Hin*dIII and *Eco*RI, the 5.2-kbp insert was separated from pBR322 sequences on agarose gel, blotted onto nitrocellulose, and hybridized to our probe. The 5.2-kbp insert of pMIA1 hybridized strongly to the 5′ rc-*mos*.

DISCUSSION

The main finding of this work is that the activation of the c-*mos* gene in XRPC24 tumor resulted from the integration of an endogenous IAP genome within the coding region of the oncogene. The mode of insertion is typical of retroviruses and transposable elements—namely, it occurred at the termini of the IAP genome and involved a duplication of the target site (6 nucleotides). The IAP genome inserted within c-*mos* consists of 4.7 kbp. It shows a high sequence homology between its LTR and the LTR of another IAP genome also involved in a rearrangement event (24). In addition, its non-LTR sequences cross-hybridize with most of the corresponding sequences found as endogenous IAP elements in the mouse genome. On the other hand, this particular genome shows variance in size and restriction enzyme sites, with a variety of IAP genomes analyzed (10, 25), including the minor population of endogenous elements reported to be transcribed and amplified in myeloma tumors (25). The *mos* sequence C-A-C-T-C-C (positions 336–341, Fig. 3) resides at the insertion junction point and was duplicated after integration of the IAP genome (see Fig. 3). Its presence (linked to an inverted repeat of the inserted element's terminus), 159 nucleotides upstream from the junction point, previously suggested that the inserted element was composed of only 159 nucleotides (8), but this now appears to be fortuitous. However, it is possible that this peculiar sequence homology directed the IAP genome to integration at the particular *mos* sequence.

Two other cases were reported in which an IAP DNA appeared in a new location within the mouse genome. In the two other events, IAP insertions into introns of κ light-chain genes resulted in the loss of gene function (26). In addition, we have recently found another mouse myeloma, in which an IAP DNA was inserted within c-*mos* (unpublished data). These findings indicate that IAP genomes appear occasionally at new sites in the cellular DNA and can affect expression of other genes. The mechanism of IAP relocation could involve a direct DNA transposition or the successive steps of transcription, reverse transcription into cDNA, and integration. Although no unintegrated IAP DNA has been found thus far in mouse myeloma (25), the retrovirus-like properties of these elements are compatible with the second mechanism described above. Moreover, two recent studies indicate that this mechanism might prove to be the general one for relocation of eukaryotic movable elements. The first work demonstrated that transcripts of copia transposable elements are associated with virion-like structures in *Drosophila* cells (27). The second study showed a striking similarity in the mode of transcription between yeast Ty1 transposable elements and retroviral DNA and suggested that Ty1 RNA might be an intermediate in the transposition of Ty1 DNA (28).

On the other hand, our study demonstrates that the two LTR of the IAP genome are not identical (Fig. 3) but contain multiple mismatches. This situation varies from the usual case of a retroviral genome where the 5′ and 3′ LTRs are essentially identical due to the unique mechanism involved in their formation by reverse transcription of the viral RNA (1). Hence, the multiple variations in the IAP LTRs would argue for insertion of the IAP genome into c-*mos* by DNA transposition rather than by integration of a reverse transcript of IAP RNA. However, it is still possible that the insertion involved a reverse transcript and the mutations in the LTR arose during the time elapsed since the establishing of the tumor line.

Certain aspects of the topography of IAP insertion bear directly on the mechanism of c-*mos* activation. The viral DNA integrated in a transcriptional orientation opposite to that of c-*mos*, placing the 5′ LTR adjacent to the main body of the gene. A consequence of the insertion was the relocation of 5′ coding and flanking DNA to a position of 4.7 kbp upstream. A schematic representation of these events is shown in Fig. 5. Subsequent to the rearrangement, transcription of the oncogene was turned on. We consider two nonexclusive mechanisms by which the turning on could have occurred. The first reflects the properties of c-*mos*. This gene appears to be under the regulation of a *cis*-acting control element located around 1 kbp upstream from the coding region (T. Wood and G. Vande Woude, personal communication). The insertion of the IAP genome has separated this element from *mos* and could have eliminated its effect on transcription of the oncogene. The second mechanism reflects the properties of the IAP LTR. Like other LTRs of retroviral genomes, it probably contains a transcriptional enhancer element (29). In fact, the two stretches of alternating purines and pyrimidines in positions 249–259 and 204–211 (Fig. 3) show a structure of Z-DNA suggested to be the critical component in enhancer elements (30). This LTR sequence, or another, could change the structure of the chromatin and increase accessibility to enzymes participating in transcription. The insertion of the IAP genome in reverse orientation precludes initiation of the 1.2-kilobase c-*mos* transcript, identified in XRPC24 cells (8), from the major viral LTR transcriptional promoter directed away from c-*mos*. Therefore, transcription presumably initiates at some other sequence of the LTR or at a cryptic site within the coding region. In both cases the transforming protein supposedly made in XRPC24 cells is expected to be significantly smaller than the corresponding M_r 37,000 protein encoded by v-*mos* (7). Identification and characterization of this protein should provide information about domains necessary for transformation or tumorigenicity (or both).

Some facets associated with the activation of c-*mos* are evident in other systems. Thus, the activation of another cellular oncogene, c-*myc*, in chicken lymphosarcomas involves the integration of an exogenous retrovirus upstream or downstream

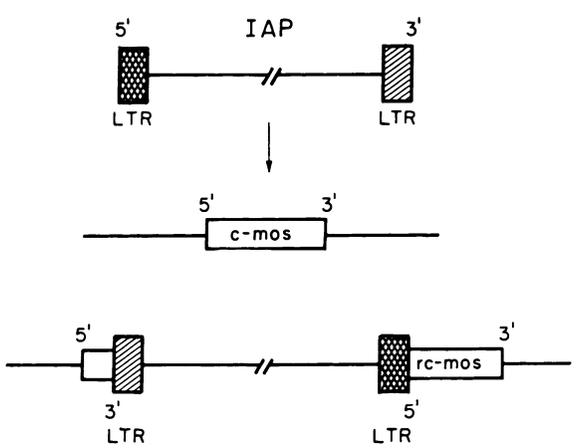

FIG. 5. Schematic representation of c-*mos* rearrangement by insertion of the IAP genome. □, c-*mos* coding region; ▨ and ▩, IAP LTRs.

from the oncogene and the subsequent enhancement of transcription through formation of a cotranscript or by another yet undefined mechanism (31, 32). Further, the activation of c-*myc* in murine plasmacytoma involves the splitting of the gene into two regions and the translocation of the fragment carrying the 3′ exons (33, 34) as well as a cryptic promoter to another region of the DNA, which presumably contains a transcriptional enhancer. Finally, the transcriptional activation of yeast genes by transposition of the Ty1 element is always characterized by insertion of the element in opposite orientation, placing its 5′ δ repeat adjacent to the activated gene (28). The significance of IAP-reversed integration and of c-*mos* splitting for activation of the oncogene could be further elucidated by *in vitro* manipulation of rc-*mos* and the detection and characterization of similar rearrangements associated with oncogenes.

We thank Dr. E. Kuff for the pMIA1 probe and for helpful discussions. This work was supported in part by grants to E.C. from the Israeli Cancer Research Fund, U.S.–Israel Binational Science Foundation, the Edith C. Blum Foundation, and the DKFZ–Israel Cancer Fund. E.C. is a fellow of the Israel Cancer Society.

1. Weiss, R., Teich, N., Varmus, H. & Coffin, S., eds. (1982) *RNA Tumor Viruses* (Cold Spring Harbor Laboratory, Cold Spring Harbor, NY).
2. Cooper, G. M. (1982) *Science* **218**, 801–806.
3. Scolnick, E. M., Howk, R. S., Anesowicz, A., Peebles, P., Sher, C. D. & Parks, W. P. (1975) *Proc. Natl. Acad. Sci. USA* **72**, 4650–4654.
4. Frankel, A. E. & Fischinger, P. J. (1976) *Proc. Natl. Acad. Sci. USA* **73**, 3705–3709.
5. Van Beveren, C., Galleshaw, S. A., Jonas, V., Berns, A. J. M., Doolittle, R. F., Donoghue, D. J. & Verma, I. M. (1981) *Nature (London)* **289**, 258–262.
6. Reddy, E. P., Smith, M. J., Canaani, E., Robbins, K. C., Tronick, S. R., Zain, S. & Aaronson, S. A. (1980) *Proc. Natl. Acad. Sci. USA* **77**, 5234–5238.
7. Papkoff, S., Verma, I. M. & Hunter, T. (1982) *Cell* **29**, 417–426.
8. Rechavi, G., Givol, D. & Canaani, E. (1982) *Nature (London)* **300**, 607–611.
9. Kuff, E. L., Feenstra, A., Lueders, K., Rechavi, G., Givol, D. & Canaani, E. (1983) *Nature (London)* **302**, 547–548.
10. Lueders, K. K. & Kuff, E. L. (1980) *Proc. Natl. Acad. Sci. USA* **77**, 3571–3575.
11. Biczysko, W., Pienkowski, M., Solter, D. & Koprowski, H. (1973) *J. Natl. Cancer Inst.* **51**, 1041–1051.
12. Calarco, P. G. & Szollosi, D. (1973) *Nature (London) New Biol.* **243**, 91–93.
13. Chase, D. G. & Piko, L. (1973) *J. Natl. Cancer Inst.* **51**, 1971–1973.
14. Dalton, A. J., Potter, M. & Merwin, R. M. (1961) *J. Natl. Cancer Inst.* **26**, 1221–1235.
15. Kuff, E. L., Lueders, K. K., Ozer, H. L. & Wivel, N. A. (1972) *Proc. Natl. Acad. Sci. USA* **69**, 218–222.
16. Maniatis, T., Fritsch, E. F. & Sambrook, S., eds. (1982) *Molecular Cloning* (Cold Spring Harbor Laboratory, Cold Spring Harbor, NY).
17. Vogelstein, B. & Gillespie, D. (1979) *Proc. Natl. Acad. Sci. USA* **76**, 615–619.
18. Leder, P., Tiemeier, D. & Enquist, L. (1977) *Science* **196**, 175–177.
19. Benton, W. D. & Davis, R. W. (1977) *Science* **196**, 180–182.
20. Maxam, A. M. & Gilbert, W. (1977) *Proc. Natl. Acad. Sci. USA* **74**, 560–564.
21. Sanger, F., Coulson, A. R., Barrell, B. G., Smith, A. J. H. & Roe, B. A. (1980) *J. Mol. Biol.* **143**, 161–178.
22. Vande Woude, G. F., Oskarsson, M., Enquist, L. W., Nomura, S., Sullivan, M. & Fischinger, P. J. (1979) *Proc. Natl. Acad. Sci. USA* **76**, 4464–4468.
23. IUPAC–IUB Commission on Biochemical Nomenclature (1968) *J. Biol. Chem.* **243**, 3557–3559.
24. Kuff, E. L., Feenstra, A., Lueders, K., Smith, L., Hawley, R., Hozumi, N. & Shulman, M. (1983) *Proc. Natl. Acad. Sci. USA* **80**, 1992–1996.
25. Shen-Ong, G. L. C. & Cole, M. D. (1982) *J. Virol.* **42**, 411–421.
26. Hawley, R. G., Shulman, M. J., Murialdo, H., Gibson, D. M. & Hozumi, N. (1982) *Proc. Natl. Acad. Sci. USA* **79**, 7425–7429.
27. Shiba, T. & Saigo, K. (1983) *Nature (London)* **302**, 119–124.
28. Elder, R. T., Loh, E. Y. & Davis, R. W. (1983) *Proc. Natl. Acad. Sci. USA* **80**, 2432–2436.
29. Yaniv, M. (1982) *Nature (London)* **297**, 17–18.
30. Nordheim, A. & Rich, A. (1983) *Nature (London)* **303**, 674–679.
31. Hayward, W. S., Neel, B. G. & Astrin, S. M. (1981) *Nature (London)* **290**, 475–480.
32. Payne, G. S., Bishop, J. M. & Varmus, H. E. (1982) *Nature (London)* **295**, 209–214.
33. Adams, J. M., Gerondakis, S., Webb, E., Corcoran, L. M. & Cory, S. (1983) *Proc. Natl. Acad. Sci. USA* **80**, 1982–1986.
34. Stanton, L. W., Watt, R. & Marcu, K. B. (1983) *Nature (London)* **303**, 401–406.